International Journal of Pharmaceutics: X 3 (2021) 100067

Contents lists available at ScienceDirect

International Journal of Pharmaceutics: X

journal homepage: www.sciencedirect.com/journal/international-journal-of-pharmaceutics-x

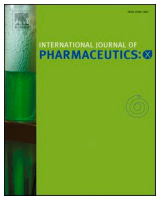

Feasibility of In-line monitoring of critical coating quality attributes via OCT: Thickness, variability, film homogeneity and roughness

Stephan Sacher [a], Anna Peter [a], Johannes G. Khinast [a,b,*]

[a] Research Center Pharmaceutical Engineering GmbH, Inffeldgasse 13/2, 8010Graz, Austria
[b] Institute for Process and Particle Engineering, Graz University of Technology, Inffeldgasse 13/3, 8010 Graz, Austria

ARTICLE INFO

Keywords:
Optical coherence tomography
In-line monitoring,tablet coating
Coating homogeneity
Coating roughness

ABSTRACT

The feasibility of Optical Coherence Tomography (OCT) for in-line monitoring of pharmaceutical film coating processes has recently been demonstrated. OCT enables real-time acquisition of high-resolution cross-sectional images of coating layers and computation of coating thickness. In addition, coating quality attributes can be computed based on in-line data. This study assesses the in-line applicability of OCT to various coating functionalities and formulations. Several types of commercial film-coated tablets containing the most common ingredients were investigated. To that end, the tablets were placed into a miniaturized perforated drum. An in-line OCT system was used to monitor the tablet bed. This set-up resembles the final stage of an industrial pan coating process. All investigated coatings were measured, and the coating thickness, homogeneity and roughness were computed. The rotation rate was varied in a range comparable to large-scale coating operations, and no influence on the outcome was observed. The results indicate that OCT can be used to determine end-point and establish in-process control for a wide range of coating formulations. The real-time computation of coating homogeneity and roughness can support process optimization and formulation development.

1. Introduction

Motivated by a shift towards continuous manufacturing in the pharmaceutical industry and the demand for more automation, in-line process monitoring and real-time process data acquisition are becoming increasingly important. Process analytical methods have been demonstrated and implemented for a range of unit operations in solid dosage manufacturing (Fonteyne et al., 2015; Laske et al., 2017). As far as the coating processes are concerned, in-process controls still mainly rely on manual measuring of the diameter or weight gain of coating thickness. This procedure is tedious and time-consuming. Moreover, it is affected by the operator's influence, involves a low number of samples and cannot account for tablet core variability.

Thus, more sophisticated methods have been reported, comprising X-ray computed tomography (XμCT) (Ariyasu et al., 2017; Radtke et al., 2019), broadband acoustic resonance dissolution spectroscopy (BARDS) (Fitzpatrick et al., 2012; Alfarsi et al., 2018), near infrared spectroscopy (NIRS) (Gendre et al., 2011; Hattori et al., 2018), Raman spectroscopy (Barimani and Kleinebudde, 2017; Kim and Woo, 2018), terahertz pulsed imaging (TPI) (May et al., 2011; Haaser et al., 2013; Lin et al., 2015a) and optical coherence tomography (OCT) (Markl et al., 2014, 2015, 2018; Sacher et al., 2019). Although XμCT offers high resolution, it is time consuming and therefore mostly used as reference method. BARDS can evaluate the coating thickness and integrity of samples drawn from the process using a correlation model. The rest of the above-mentioned methods are capable of measuring the coating properties in-line. While calibration models are required for NIR and Raman spectroscopy, TPI and OCT can measure the coating thickness directly. In addition to offering high resolution, TPI and OCT can measure coating properties of single-dosage units (Lin et al., 2017a). Especially OCT, which is based on low coherence interferometry, is suitable for monitoring the coating quality in real time due to its high acquisition rate (Sacher et al., 2019). Coating homogeneity and coating roughness can be computed in real time. The drawback of OCT is a lower penetration depth compared to TPI (Lin et al., 2015b). Scattering particles can limit the penetration and hinder the coating layer detection. However, a wide range of functional coating formulations can be analyzed by means of OCT. Lin et al. (2017b) investigated the applicability of OCT to common coating materials in the off-line mode. Wolfgang et al. (2019) demonstrated the validity of OCT results for at-line and in-line applications using a polymer reference target as well as coated tablets and complementary methods.

* Corresponding author at: Research Center Pharmaceutical Engineering GmbH, Inffeldgasse 13/2, 8010Graz, Austria.
E-mail address: khinast@tugraz.at (J.G. Khinast).

https://doi.org/10.1016/j.ijpx.2020.100067
Received 25 September 2020; Received in revised form 10 December 2020; Accepted 11 December 2020
Available online 17 December 2020

However, all studies on the applicability of OCT for analysis of different coating formulations so far concentrated on off-line OCT technology. Therefore, in this study we investigate the feasibility of an in-line OCT system for analysis of common coating formulations. As a model setup, the coating process was experimentally simulated using a perforated rotating drum, which enables the same measurement conditions as an industrial scale pan coater. This drum is commercially used as an at-line monitoring system, as it mimics a modern drum coater in terms of tablet bed movement and monitoring characteristics. Several types of commercially-available coated tablets were investigated. In addition to coating thickness, for the first time homogeneity and roughness were computed for commercial tablet formulations based on

Table 1
Tablets, coating ingredients and coating functionality.

Brand name	Film-forming polymer	Plasticiser	Other ingredients	Coating functionality	Tablet shape	Tablet size (round: d x h, oval: l x w x h) [mm]	Tablet photo (not to scale)
RatioDolor	HPMC	PEG, Glycerol		Cosmetic	Oval	19.3 × 8.3 × 5.3	
Glucophage	HPMC			Cosmetic	Round, biconvex	13.6 × 6.6	
Zinkorotat POS	Eudragit L	Triethyl citrate	Talcum	Delayed release	Round, biconvex	9.3 × 4.9	
Thrombo ASS	Eudragit L	Triacetin	Talcum	Delayed release	Round, biconvex with small bevel edge	7.3 × 4	
Pantoloc	HPMC, PVP Eudragit L30D	Propylene glycol Triethyl citrate	Titanium dioxide, yellow iron oxide Yellow, red and black iron oxide	Inner layer, isolation Top layer delayed release	Oval, biconvex	11.7 × 6 × 4	
Pantoprazol	HPMC Eudragit L30D	Triethyl citrate Triethyl citrate	SCMS Yellow iron oxide	Inner layer, isolation Top layer delayed release	Oval, biconvex	9.3 × 4.9	
Pharm 1	HPMC, CA	PEG	Opadry, Opacode black ink	Osmotic release (controlled release)	Round, biconvex	8 × 4	
Pharm 2	HPMC, CA	PEG		Osmotic release (controlled release)	Round, biconvex	11.3 × 6	
Pharm 3	HPMC, CA, hydroxypropyl cellulose	PEG, Triacetin		Extended release	Oval, biconvex	10.8 × 5.5 × 4.4	

HPMC = hydroxypropyl methylcellulose, CA = cellulose acetate, PEG = polyethylene glycol, PVP = polyvinylpyrrolidon, SCMS = sodium carboxymethyl starch, d = tablet diameter, h = tablet height, l = tablet length, w = tablet width.

data acquired in real time.

2. Materials and methods

2.1. Tablet core and coating material

Commercial tablets with different coating formulations were purchased in a standard pharmacy. In addition, three types of tablets were supplied by a pharmaceutical company (hereinafter referred to as Pharm 1, Pharm 2 and Pharm 3 rather than by the brand name). The coatings of the investigated tablets contain mostly common polymers and represent most types of coating functionalities, i.e., cosmetic, delayed release (enteric), extended release and osmotic-controlled release. The cosmetic coatings contained hydroxypropyl methylcellulose (HPMC) as a film-forming polymer, and the delayed release coatings were Eudragit-based. Both Eudragit L and Eudragit L30D are co-polymers of methacrylic acid with methyl acrylate and ethyl acrylate, respectively. The osmotic release coatings in this study contained HPMC and cellulose acetate (CA) as a polymer, and the extended release coating contained hydroxypropyl cellulose in addition. The coating of two types of tablets (Pantoloc and Pantoprazol) consisted of two separate layers, which may pose a challenge to the monitoring technique. Only tablets without or with a low amount of scattering pigments were selected, as high pigment contents is a limitation for OCT (Lin et al., 2017b). The tablets had round biconvex and oval biconvex shapes and sizes from 7 mm to 19 mm in diameter or length. Table 1 provides an overview of the investigated tablets and their most important coating ingredients. The dimensions were measured with a calliper. Note that pictures in the Table are not on the same scale.

2.2. Optical coherence tomography measurements

The tablets were filled into an at-line tablet sampling device (Phyllon, Austria) and presented to the OCT probe. This system contained a perforated rotating drum with variable rotation rate, which mimicked an industrial scale pan coater and had holes with a diameter of 2.8 mm and has the advantage that a few hundred tablets can be analyzed at the same time. An in-line OCT sensor (OSeeT Pharma 1D, Phyllon, Austria) was placed below the drum and measured the passing tablets through the holes in the drum in the same way as in an industrial application described in Markl et al. (2015). A front cover of Plexiglas made it possible to watch the tablets moving. Fig. 1 shows an image of the at-line sampling device in operation, filled with a bed of tablets. For better visibility of the tablets in the image, the Plexiglas cover of the device was dismantled.

The tablets were placed into the perforated drum. Either 200 or a minimum of 100 ml of tablets were filled depending on the tablet size in order to achieve a uniform tablet bed. For the pan diameter of 0.2 m, a rotation speed of 30 rpm was adjusted to achieve a circumferential speed of 0.31 m/s. This resembles the operating conditions in an industrial-scale pan coater with pan diameters from 0.6 m to 0.8 m, which typically operates at 8–10 rpm (Wang et al., 2012).

For OCT measurements, the spectral-domain (SD) system described in Sacher et al. (2019) was used. It consists of a base unit (which houses the light source, the spectrometer and the electronics) and the sensor head, which divides the light beam into the measurement and reference beams. As light source a super luminescent diode (SLD, BLMS mini, Superlum Diodes Ltd., Ireland) with a central wavelength of 832 nm and spectral full-width at half-maximum (FWHM) bandwidth of 75 nm was used. The resulting axial resolution in air is 4 µm. The system acquires up to 100,000 single depth scans (A-scans) per second. The sensor head was placed into the at-line sampling device and connected to the base unit via an optical glass fibre. For image evaluation, the algorithm presented in Sacher et al. (2019) was applied. First, each A-scan is classified into the categories air, tablet and drum. Next, the interfaces between the air and the coating and between the coating and the core are detected via ellipse fitting. The coating thickness is computed as the shortest distance between the ellipse fits of air/coating and coating/core interfaces perpendicular to the top interface. To exactly identify an interface, three adjacent layers must be clearly visible in the OCT image. Taking the axial resolution of 4 µm into account, this results in a detection limit of 12 µm. The coating homogeneity is calculated as a ratio between the number of pixels with brightness above a defined value and the total number of pixels in the detected coating layer. Therefore, a more uniform coating layer with fewer dark pixels yields a higher homogeneity value. The coating roughness is defined as a root mean squared error (RMSE) between the real top interface peaks and the ideal top interface ellipse. All coating properties are computed based on the acquired depth profiles in real time. Fig. 2 shows how the thickness (distance between the ellipse fits in red), the coating homogeneity (calculated using all pixel data within the ellipse fits and the vertical lines) and the coating roughness (deviation between the upper ellipse fit and the true coating surface in the cross section) are defined.

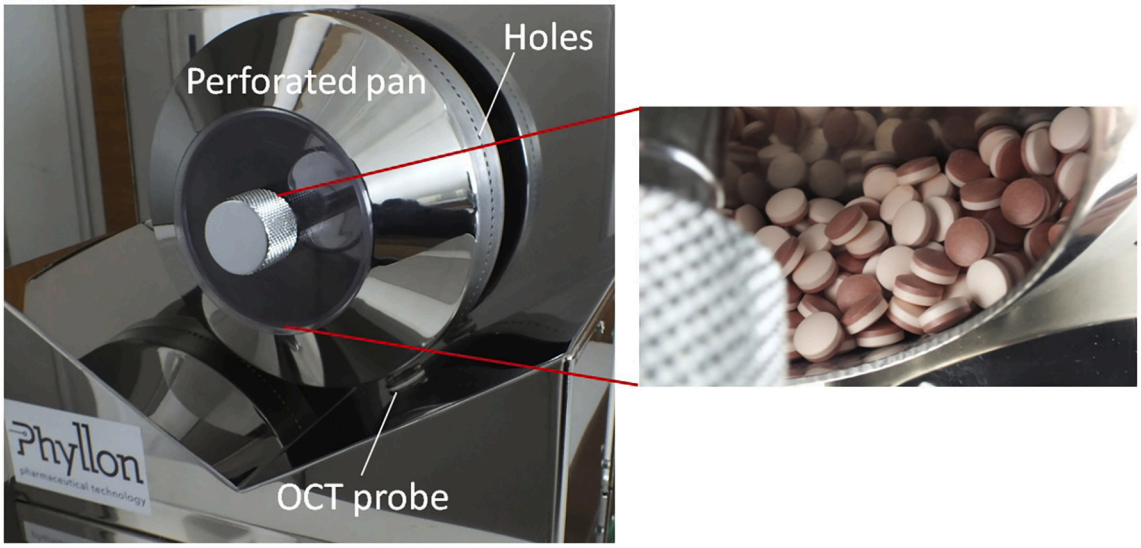

Fig. 1. At-line sampling device with a rotating drum and an in-line OCT sensor. The insert shows the moving tablet bed in the drum.

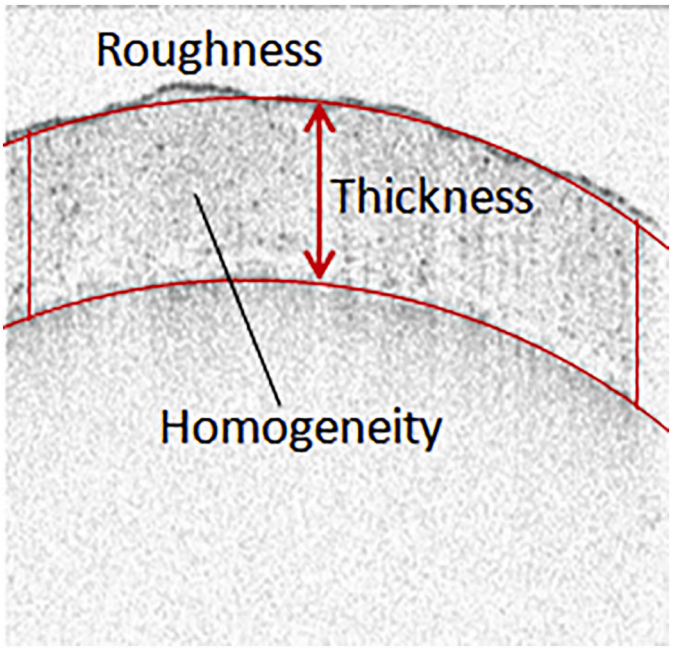

Fig. 2. Definition of coating thickness, homogeneity and roughness.

2.3. Reference analytics

The tablet coating layers were investigated off-line via light microscopic (LM) imaging. From each tablet type, 10 tablets were selected randomly for LM analysis from the tablets, which have also been measured in the at-line sampling device before. In the case of circular or oblong shape, the tablets were cut with a sharp knife on one convex side between the center and the outer edge. Capsule-shaped tablets were cut in the center on one side in the circumferential direction. After cutting off half of the tablet height, all tablets were broken manually. This procedure allowed an optimal preservation of the coating layer. The broken sides of the tablets were analyzed by means of a light microscope (Leica DM 4000 M from Leica, Germany) with a 50-fold magnification in the reflectance mode. The coating thickness was measured in 10 positions for each tablet using the software Leica Application Suite v4.9. An error of 10% was estimated based on the range of subjective identification of the layer boundaries. Images with 200-fold magnification were taken to acquire an optical impression of the coating homogeneity.

3. Results and discussion

The OCT images were acquired by means of in-line OCT system and the coating attributes were computed in real-time. A refractive index of 1.5 was assumed for all investigated coatings. Since coating polymers typically have refractive indices between 1.4 and 1.6 in the wavelength range of the applied OCT system (https://refractiveindex.info, 2020), the potential maximum deviation for the coating thickness is 7%, compared to the value obtained via the actual refractive index.

If OCT is employed in industrial applications, the actual refractive index should be used to obtain the most accurate coating thickness. Although the residual moisture content in the coating layer can influence the refractive index, it can be assumed to be constant for tablets at the outer region of the coater close to the drum, where an in-line OCT measurement is performed from outside the coater through the holes of the drum. However, for end-point determination, in-process control and closed-loop process control, establishing a relative increase in the coating thickness and the value related to the optimal drug dissolution performance is sufficient. In Fig. 3, OCT images of the investigated commercial tablet coatings, acquired via the in-line OCT system, are shown. The orientation of the coating layers in the images depends on the orientation of the tablet in front of the OCT sensor. The green areas represent the sections of the layer that are classified as coatings by the algorithm. Based on these image data, the coating attributes are computed. The scale bar shows the dimension in the direction of light beam in the z-axis. The dimension in the x-axes depends on the speed of the tablets passing in front of the light beam and on the pan speed. The coating layers of all investigated tablets were successfully detected and classified, from very thin (15 µm at RatioDolor) to very thick coating layers (158 µm at Pantoprazol).

Interestingly, even coating layers with lower amounts of talcum or iron oxides could be detected (see Table 1), while titanium dioxide disabled proper layer identification. Only the top layers of Pantoloc and Pantoprazol could be detected. In contrast, in the LM images of these tablets, two layers are visible. Fig. 4 shows light microscopic images of all investigated tablet coatings with a 200-fold magnification. For Pantoloc, both layers are in the same thickness range, while for Pantoprazol the inner layer is very thin. A potential reason could be that the amount of titanium dioxide in the inner layer of Pantoloc hinders proper detection of the second layer via OCT. Another cause could be overlap or penetration of the core and the isolation layer, making the detection of a distinct interface impossible.

Table 2 summarizes the coating attributes and their relative standard deviations (RSD) based on 500 OCT detections. In addition, the mean coating thicknesses and RSDs from analysis of the LM images are provided, based on approximately 100 measurements in different positions on the tablets, including band and bend. The values for RatioDolor and Glucophage are missing since their coating layers were too thin for a reliable evaluation based on the LM images.

Fig. 5 shows an example of the thickness measurements based on the LM images. The mean coating thicknesses of OCT and LM are in very good agreement for most of the tablets. Potential reasons for the relative thickness deviation between OCT and LM are the difference between the estimated and the actual refractive indexes and the challenge of manually selecting the correct interfaces in the LM images. However, it is below 5% for all tablets, except for Pharm 2 and Pharm 3, which show deviations in the range of 10%. Assessing the measurements in more detail reveals that the majority of thicker LM readings stem from positions far away from the tablet center. In contrast, OCT acquires its data more often from the top of the tablets due to their orientation in the drum. We thus, conclude that for these tablets (Pharm 2 and 3) the coating thickness is not evenly distributed. For Pantoloc and Pantoprazol only the top layer values are shown in Table 2.

The RSD of the coating thickness is below 15% for most tablet samples. It has been shown in the literature that the coating thickness can vary greatly between tablets (inter-tablet variability) (Sacher et al., 2019; Wahl et al., 2019; Lin et al., 2017a) due to the randomly distributed amount of spray being deposited on each tablet and, to a certain extent, to the uneven surface of tablet cores. For two tablets (Glucophage and Thrombo ASS), the RSD is higher. Since the formulations of these two tablets are different, yet similar to other tablets with lower RSD, their broad RSD rather seems to stem form the process. Due to a relatively small number of measurements, the RSD based on LM can only be used to estimate tendencies in the thickness variation. These are, however, comparable to the OCT results.

The coating homogeneity, which represents the number of dark pixels related to the overall number of pixels in the coating layer, varies greatly among the investigated tablets and seems to be related to the type of coating and ingredients. Products that contain HPMC have high homogeneity values, while the Eudragit-based coatings have low homogeneity (as reflected by the darker images in Fig. 3). The coatings of Ratiodolor and Glucophage are very thin. For a thin coating layer, the air-coating and coating-core interfaces, which also consist of dark pixels, can influence the computation of homogeneity. Therefore, these two tablets were excluded from the comparison. The homogeneity acquired via OCT is influenced by a change in the refractive index within the

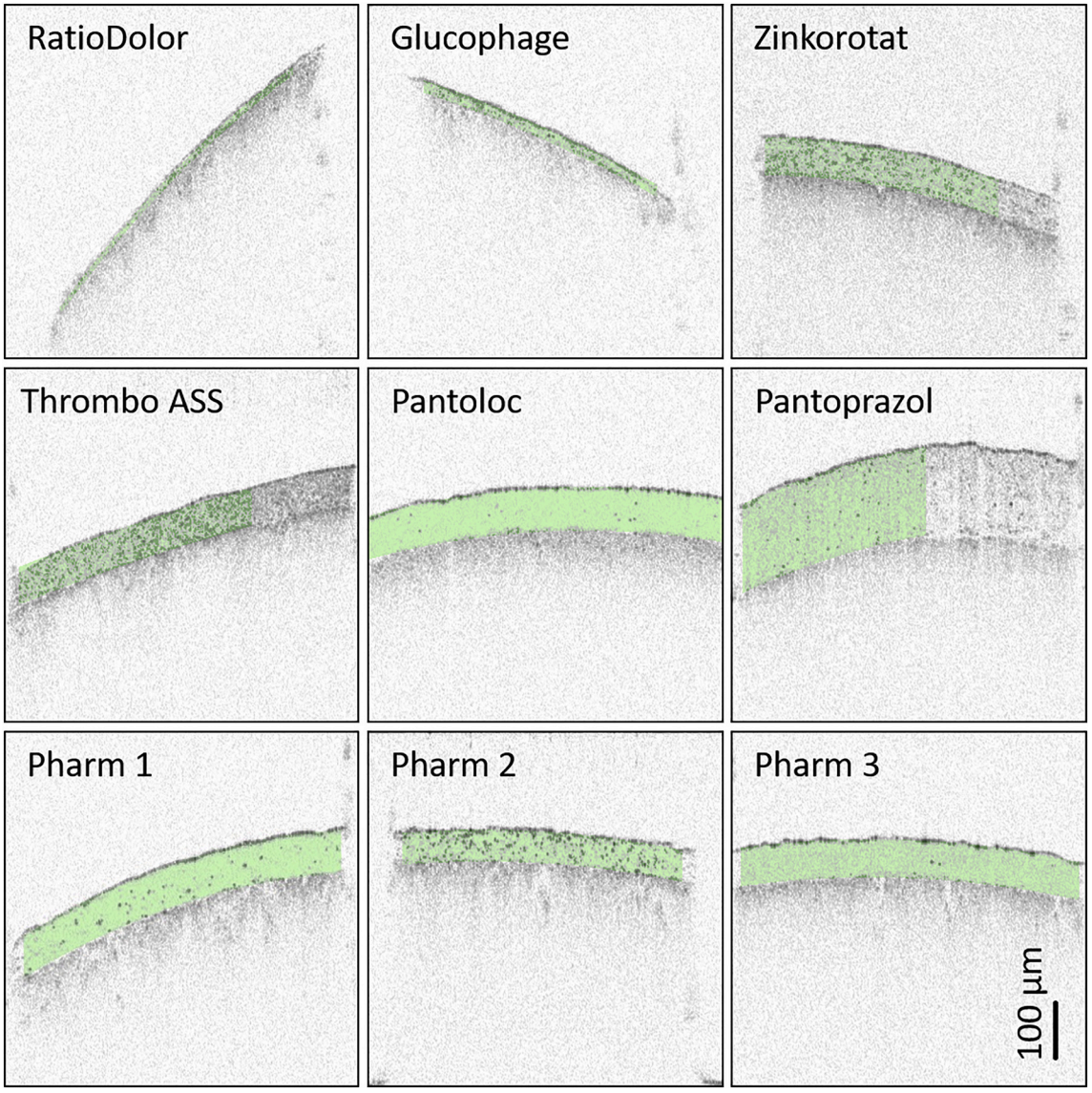

Fig. 3. Images of commercial tablet coatings acquired using the OCT in-line sensor. The scale bar represents the coating layer dimension.

coating layer, which can be caused by any kind of inclusions and a different amount of residual solvent during drying and curing that are affected by both the formulation and the process. OCT has the potential to analyze and detect deviations in the coating homogeneity from a predefined set-point, and to support formulation development and process control. The dark pixels in the images of the osmotic release products Pharm 1 and Pharm 2 can be due to porosity in these coating formulations. Therefore, the homogeneity could also be used as an indicator of the layer porosity.

The LM images in Fig. 4 provide further information about the internal coating structure, although they show a very limited area. Pantoloc with the highest homogeneity computed via OCT has a very smooth and uniform coating layer, while Zinkorotat POS and Thrombo ASS with the lowest OCT homogeneity have the most irregular coating appearance. Thus, there is a clear correlation between visual appearance and the measured OCT homogeneity. In the LM images of Pantoprazol, some grains or inclusions can be found, which result in a lower homogeneity compared to Pantoloc. This is in agreement with OCT. However, the LM images of Pharm 1, Pharm 2 and Pharm 3 leave room for interpretation. While the OCT homogeneities of Pharm 1 and Pharm 3 are close to Pantoloc, the LM images indicate a layered coating structure similar to Zinkorotat. This may reflect layer-wise application and drying during the coating process. To the naked eye, the coating structure of Pharm 2 looks similar, although the homogeneity is much lower. A potential reason of grain-like or irregular areas of coating, which is not clearly related to the formulation or the process, is the preparation procedure that can induce delamination of the coating. Compared to the coating structure analysis via LM, OCT provides a more objective representation based on the number of pixels darker than a defined threshold. Nevertheless, the homogeneity value computed by OCT can be influenced by various sources (real change in homogeneity due to process or formulation, but also image artefacts due to broader dark areas at layer interfaces) and therefore, more research on this topic is needed.

The coating roughness is 3–4 µm for most of the investigated samples. Only the thin coating layers of Ratiodolor and Glucophage show less roughness. This is in good agreement with the observation that the coating roughness increases with increasing process time (Sacher et al., 2019; Seitavuopio et al., 2006). The roughness of Pantoprazol's very thick coating is still about 4 µm. This correlates with Seitavuopio et al. (2006), who found that the coating roughness increases in the beginning of the coating process and remains stable after some period of process time leading to no further increase for thick coatings. The absolute roughness values are within the same range as those obtained via

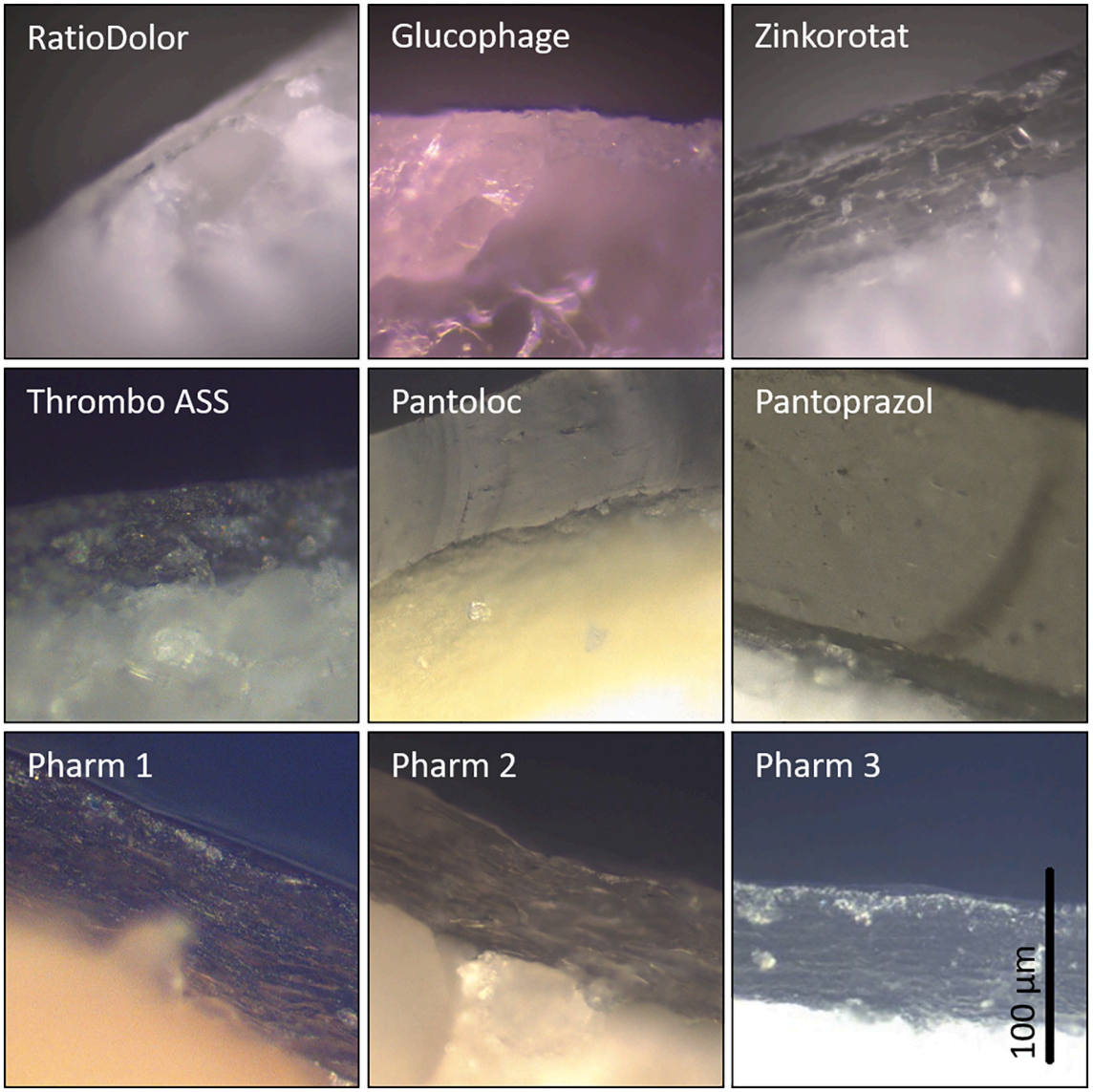

Fig. 4. Images of commercial tablet coatings acquired using the light microscope in the reflectance mode with 200 fold magnification.

contact profilometry (Markl et al., 2018) and laser scanning microscope (Dohi et al., 2016).

The OCT measurements were repeated at various rotation rates to investigate the influence of tablet speed on the quality of the results. As a lower limit, a rotation rate of 20 rpm was selected. At this speed, there is still enough movement in the tablet bed to induce sufficient exchange of tablets in front of the OCT sensor. The upper limit of 40 rpm still provides a bed of tablets, while a further increase in the drum speed leads to cascading and tumbling of tablets in the drum. Depending on the size and shape of tablets, slightly lower and higher drum speeds are possible. The investigated range also represents typical operation states of conventional coaters. Generally, faster movement of the tablets in front of the OCT sensor leads to distortions in the acquired images (Markl et al., 2014). This effect can be overcome by decreasing the time between two A-scan acquisitions and obtaining more information for each tablet. In this study, exactly the same settings of the OCT system were used for all rotation rates. The results in Table 2 indicate that a change in the rotation rate within the described limits does not influence the OCT readings. The measured coating thickness remained within a range of ±1 µm. Coating homogeneity and roughness are not affected significantly by an altered drum rotation either, meaning that the operator can run OCT at a wide range of coater speeds using the same settings.

4. Conclusion

When applying OCT for in-line monitoring of industrial coating processes, it is essential to establish which type of coatings can be measured. In this study, several types of tablets containing common coating polymers and plasticisers were investigated using an in-line OCT system. All tested materials could be measured and coating attributes computed in real time, from very thin coating layers of about 15 µm to very thick coating layers of over 150 µm. Although coatings with high pigment scattering were excluded from the study, it was possible to detect the coating layer interfaces for drug products with fewer pigments. In addition to the coating thickness, homogeneity and roughness could be computed based on the OCT images. Homogeneity is linked to the coating formulation, while roughness seems to be influenced mainly by the process. OCT has high potential to support formulation development and process optimization via coating quality monitoring. Compared to LM imaging, OCT can provide statistically more representative information about the coating structure much faster. However, deeper investigation of both of these coating attributes is required to understand the link between coating quality and effects such as drying and curing.

The results of this study are valid for coating processes on the

Table 2
Tablet coating attributes computed using the OCT data and coating thickness obtained via light microscopic (LM) imaging.

Tablet	at 20 rpm			at 30 rpm			at 40 rpm			LM
	Mean Coating Thickness [µm] and RSD	Mean Coating Homogeneity [%] and RSD	Mean Coating Roughness [µm] and RSD	Mean Coating Thickness [µm] and RSD	Mean Coating Homogeneity [%] and RSD	Mean Coating Roughness [µm] and RSD	Mean Coating Thickness [µm] and RSD	Mean Coating Homogeneity [%] and RSD	Mean Coating Roughness [µm] and RSD	Mean Coating Thickness [µm] and RSD
RatioDolor	15.5 ± 14.7	41.9 ± 50.6	1.9 ± 24.5	15.5 ± 13.6	34.6 ± 53.5	1.9 ± 20.1	15.7 ± 13.3	42.6 ± 44.9	1.9 ± 50.4	–
Glucophage	21.5 ± 24.7	41.9 ± 39.4	1.4 ± 15.0	20.7 ± 21.3	55.9 ± 29.0	1.4 ± 11.3	19.9 ± 20.1	50.0 ± 32.4	1.4 ± 11.1	–
Zinkorotat POS	63.9 ± 13.5	57.2 ± 37.2	3.3 ± 52.5	64.2 ± 12.8	55.8 ± 33.4	3.4 ± 50.7	63.5 ± 12.4	62.9 ± 27.6	3.3 ± 46.5	67.2 ± 6.8
Thrombo ASS	52.2 ± 19.7	51.9 ± 47.6	3.7 ± 43.1	50.5 ± 15.2	49.3 ± 47.6	3.6 ± 38.1	51.2 ± 15.0	49.7 ± 44.7	3.7 ± 36.4	50.1 ± 15.5
Pantoloc	77.5 ± 12.3	98.2 ± 1.5	2.9 ± 57.1	76.2 ± 11.9	97.9 ± 1.8	3.4 ± 47.6	76.0 ± 12.6	97.9 ± 1.9	3.8 ± 49.8	73.7 ± 14.9
Pantoprazol	156.2 ± 11.3	86.5 ± 7.3	5.3 ± 60.7	157.8 ± 11.1	86.4 ± 5.8	4.1 ± 62.1	157.1 ± 11.6	89.2 ± 6.3	5.4 ± 63.8	162.4 ± 7.8
Pharm1	79.3 ± 11.6	96.0 ± 3.7	4.0 ± 57.0	78.5 ± 11.0	95.9 ± 2.6	3.4 ± 55.0	77.9 ± 11.0	96.5 ± 2.9	3.7 ± 56.4	81.6 ± 8.1
Pharm2	58.7 ± 13.2	81.1 ± 6.8	4.6 ± 28.1	58.6 ± 11.9	82.2 ± 5.8	4.3 ± 28.1	59.9 ± 12.2	84.6 ± 4.9	4.2 ± 28.9	63.8 ± 8.2
Pharm3	75.3 ± 11.4	92.9 ± 6.7	3.2 ± 52.9	74.3 ± 10.5	94.1 ± 5.1	3.2 ± 47.2	74.4 ± 10.8	94.1 ± 4.6	3.6 ± 47.5	82.6 ± 7.7

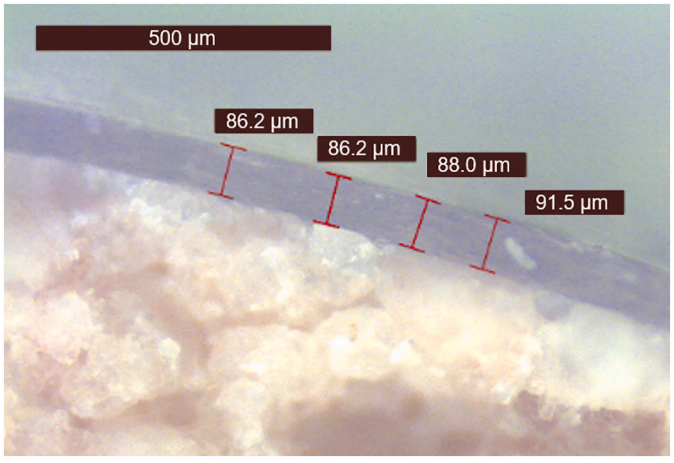

Fig. 5. Coating thickness measurement in the LM image.

industrial scale since the conditions in the miniaturized drum set-up mimicked large-scale drum coating. Therefore, OCT is applicable for end-pint determination and in-process monitoring of a wide range of pharmaceutical coatings. To maximize the use of OCT capabilities, future work must concentrate on implementation in industrial-scale processes and combination with process control systems. Development of closed-loop control based on a correlation between coating attributes monitored by OCT and critical quality attributes of the drug product will support manufacturing of precise coating applications.

Declaration of Competing Interest

The authors declare that they have no known competing finanicial interests or personal relationships that could have appeared to influence the work reported in this paper.

Acknowledgements

This work was funded by the Austrian COMET Program under the auspices of the Austrian Federal Ministry of Transport, Innovation and Technology (bmvit), the Austrian Federal Ministry of Economy, Family and Youth (bmwfj) and by the State of Styria (Styrian Funding Agency SFG). COMET is managed by the Austrian Research Promotion Agency FFG.

References

https://refractiveindex.info, 2020 accessed on 7.12.2020.

Alfarsi, A., Dillon, A., McSweeney, S., Krüse, J., Griffin, B., Devine, K., Sherry, P., Henken, S., Fitzpatrick, S., Fitzpatrick, D., 2018. Broadband acoustic resonance dissolution spectroscopy (BARDS): a rapid test for enteric coating thickness and integrity of controlled release pellet formulations. Int. J. Pharm. 544, 31–38. https://doi.org/10.1016/j.ijpharm.2018.04.018.

Ariyasu, A., Hattori, Y., Otsuka, M., 2017. Non-destructive prediction of enteric coating layer thickness and drug dissolution rate by near-infrared spectroscopy and X-ray computed tomography. Int. J. Pharm. 525, 282–290. https://doi.org/10.1016/j.ijpharm.2017.04.017.

Barimani, S., Kleinebudde, P., 2017. Evaluation of in-line Raman data for end-point determination of a coating process: Comparison of science-based calibration, PLS-regression and univariate data analysis. Eur. J. Pharm. Biopharm. 119, 28–35. https://doi.org/10.1016/j.ejpb.2017.05.011.

Dohi, M., Momose, W., Yoshino, H., Hara, Y., Yamashita, K., Hakomori, T., Sato, S., Terada, K., 2016. Application of terahertz pulse imaging as PAT tool for non-destructive evaluation of film-coated tablets under different manufacturing conditions. J. Pharm. Biomed. Anal. 119, 104–113. https://doi.org/10.1016/j.jpba.2015.11.046.

Fitzpatrick, D., Kruse, J., Vos, B., Foley, O., Gleeson, D., O'Gorman, E., O'Keefe, R., 2012. Principles and applications of broadband acoustic resonance dissolution spectroscopy (BARDS): a sound approach for the analysis of compounds. Anal. Chem. 84 (5), 2202–2210. https://doi.org/10.1021/ac202509s.

Fonteyne, M., Vercruysse, J., De Leersnyder, F., Van Snick, B., Vervaet, C., Remon, J.P., De Beer, T., 2015. Process Analytical Technology for continuous manufacturing of solid-dosage forms. Trends Anal. Chem. 67, 159–166. https://doi.org/10.1016/j.trac.2015.01.011.

Gendre, C., Genty, M., Boiret, M., Julien, M., Meunier, L., Lecoq, O., Baron, M., Chaminade, P., Péan, J.M., 2011. Development of a Process Analytical Technology (PAT) for in-line monitoring of film thickness and mass of coating materials during a pan coating operation. Eur. J. Pharm. Sci. 43, 244–250. https://doi.org/10.1016/j.ejps.2011.04.017.

Haaser, M., Gordon, K.C., Strachan, C.J., Rades, T., 2013. Terahertz pulsed imaging as an advanced characterisation tool forfilm coatings—a review. J. Pharm. Sci. 106, 3171–3176. https://doi.org/10.1016/j.xphs.2017.05.032.

Hattori, Y., Sugata, M., Kamata, H., Nagata, M., Nagato, T., Hasegawa, K., Otsuka, M., 2018. Real-time monitoring of the tablet-coating process by near-infrared spectroscopy - Effects of coating polymer concentrations on pharmaceutical properties of tablets. J. Drug Deliv. Sci. Techn. 46, 111–121. https://doi.org/10.1016/j.jddst.2018.04.018.

Kim, B., Woo, Y.-A., 2018. Coating process optimization through in-line monitoring for coatingweight gain using Raman spectroscopy and design of experiments. J. Pharm. Biomed. Anal. 154, 278–284. https://doi.org/10.1016/j.jpba.2018.03.001.

Laske, S., Paudel, A., Scheibelhofer, O., et al., 2017. A review of PAT strategies in secondary solid oral dosage manufacturing of small molecules. J. Pharm. Sci. 106, 667–712. https://doi.org/10.1016/j.xphs.2016.11.011.

Lin, H., May, R.K., Evans, M.J., Zhong, S., Gladden, L.F., Shen, Y., Zeitler, J.A., 2015a. Impact of processing conditions on inter-tablet coating thickness variations measured by terahertz in-line sensing. J. Pharm. Sci. 104, 2513–2522. https://doi.org/10.1002/jps.24503.

Lin, H., Dong, Y., Shen, Y., Zeitler, J.A., 2015b. Quantifying pharmaceutical film coating with optical coherencetomography and terahertz pulsed imaging: an evaluation. J. Pharm. Sci. 104, 3377–3385. https://doi.org/10.1002/jps.24535.

Lin, H., Dong, Y., Markl, D., Williams, B.M., Zheng, Y., Shen, Y., Zeitler, J.A., 2017a. Measurement of the intertablet coating uniformity of a pharmaceutical pan coating process with combined terahertz and optical coherence tomography in-line sensing. J. Pharm. Sci. 106, 1075–1084. https://doi.org/10.1016/j.xphs.2016.12.012.

Lin, H., Dong, Y., Markl, D., Zhang, Z., Shen, Y., Zeitler, J.A., 2017b. Pharmaceutical film coating catalog for spectral domain optical coherence tomography. J. Pharm. Sci. 106, 3171–3176. https://doi.org/10.1016/j.xphs.2017.05.032.

Markl, D., Hannesschläger, G., Buchsbaum, A., Sacher, S., Khinast, J.G., Leitner, M., 2014. In-line quality control of moving objects by means of spectral-domain OCT. Optics Lasers Eng. 59, 1–10. https://doi.org/10.1016/j.optlaseng.2014.02.008.

Markl, D., Hannesschläger, G., Sacher, S., Leitner, M., Buchsbaum, A., Pescod, R., Baele, T., Khinast, J.G., 2015. In-line monitoring of a pharmaceutical pan coating process by optical coherence tomography. J. Pharm. Sci. 104, 2531–2540. https://doi.org/10.1002/jps.24531.

Markl, D., Wahl, P., Pichler, H., Sacher, S., Khinast, J.G., 2018. Characterization of the coating and tablet core roughness by means of 3D optical coherence tomography. Int. J. Pharm. 536, 459–466. https://doi.org/10.1016/j.ijpharm.2017.12.023.

May, R.K., Evans, M.J., Zhong, S., Warr, I., Gladden, L.F., Shen, Y., Zeitler, J.A., 2011. Terahertz in-line sensor for direct coating thickness measurement of individual tablets during film coating in real-time. J. Pharm. Sci. 100, 1535–1544. https://doi.org/10.1002/jps.22359.

Radtke, J., Wiedey, R., Kleinebudde, P., 2019. Effect of coating time on inter- and intra-tablet coating uniformity. Eur. J. Pharm. Sci. 137, 104970. https://doi.org/10.1016/j.ejps.2019.104970.

Sacher, S., Wahl, P., Weißensteiner, M., Wolfgang, M., Pokhilchuk, Y., Looser, B., Thies, J., Raffa, A., Khinast, J.G., 2019. Shedding light on coatings: Real-time monitoring of coating quality atindustrial scale. Int. J. Pharm. 566, 57–66. https://doi.org/10.1016/j.ijpharm.2019.05.048.

Seitavuopio, P., Heinämäki, J., Rantanen, J., Yliruusi, J., 2006. Monitoring tablet surface roughness during the film coating process. AAPS PharmSciTech 7, 31. https://doi.org/10.1208/pt070231.

Wahl, P., Peter, A., Wolfgang, M., Khinast, J.G., 2019. How to measure coating thickness of tablets: Method comparison of optical coherence tomography, near-infrared spectroscopy and weight-, height- and diameter gain. Eur. J. Pharm. Biopharm. 142, 344–352. https://doi.org/10.1016/j.ejpb.2019.06.021.

Wang, J., Hemenway, J., Chen, W., Desai, D., Early, W., Paruchuri, S., Chang, S.-Y., Stamato, H., Varia, S., 2012. An evaluation of process parameters to improve coating efficiency of an active tablet film-coating process. Int. J. Pharm. 427, 163–169. https://doi.org/10.1016/j.ijpharm.2012.01.033.

Wolfgang, M., Peter, A., Wahl, P., Markl, D., Zeitler, J.A., Khinast, J.G., 2019. At-line validation of optical coherence tomography as in-line/at-line coatingthickness measurement method. Int. J. Pharm. 572, 118766. https://doi.org/10.1016/j.ijpharm.2019.118766.